

Vision-Language Pre-training with Object Contrastive Learning for 3D Scene Understanding

Taolin Zhang^{1*}, Sunan He^{1*}, Tao Dai^{2✉}, Bin Chen³, Zhi Wang² and Shu-Tao Xia^{1,4}

¹Tsinghua Shenzhen International Graduate School, Tsinghua University

²College of Computer Science and Software Engineering, Shenzhen University

³Harbin Institute of Technology, Shenzhen

⁴Research Center of Artificial Intelligence, Peng Cheng Laboratory

{zhangtlin3,daitao.edu}@gmail.com,{hsn20,wangzhi}@mails.tsinghua.edu.cn,chenbin2021@hit.edu.cn,xiast@sz.tsinghua.edu.cn

ABSTRACT

In recent years, vision language pre-training frameworks have made significant progress in natural language processing and computer vision, achieving remarkable performance improvement on various downstream tasks. However, when extended to point cloud data, existing works mainly focus on building task-specific models, and fail to extract universal 3D vision-language embedding that generalize well. We carefully investigate three common tasks in semantic 3D scene understanding, and derive key insights into the development of a pre-training model. Motivated by these observations, we propose a vision-language pre-training framework 3DVLP (3D vision-language pre-training with object contrastive learning), which transfers flexibly on 3D vision-language downstream tasks. 3DVLP takes visual grounding as the proxy task and introduces Object-level IoU-guided Detection (OID) loss to obtain high-quality proposals in the scene. Moreover, we design Object-level Cross-Contrastive alignment (OCC) task and Object-level Self-Contrastive learning (OSC) task to align the objects with descriptions and distinguish different objects in the scene, respectively. Extensive experiments verify the excellent performance of 3DVLP on three 3D vision-language tasks, reflecting its superiority in semantic 3D scene understanding.

CCS CONCEPTS

• **Computing methodologies** → **Computer vision**; **Natural language processing**; **Neural networks**.

KEYWORDS

3D vision-language tasks, model pre-training, contrastive learning

1 INTRODUCTION

Semantic 3D scene understanding has recently attracted increasing research interest due to its wide applications such as automatic driving, human-machine interaction, *etc.* Much progress has been made in semantic 3D scene understanding, with task-specific models continuously pushing the state-of-the-art in various downstream tasks including visual grounding [6, 7, 48], dense captioning [11], and question answering [3].

While effective on their respective benchmarks, the task-specific representations obtained by existing approaches prevent them from generalizing well to other tasks. A common practice for extracting

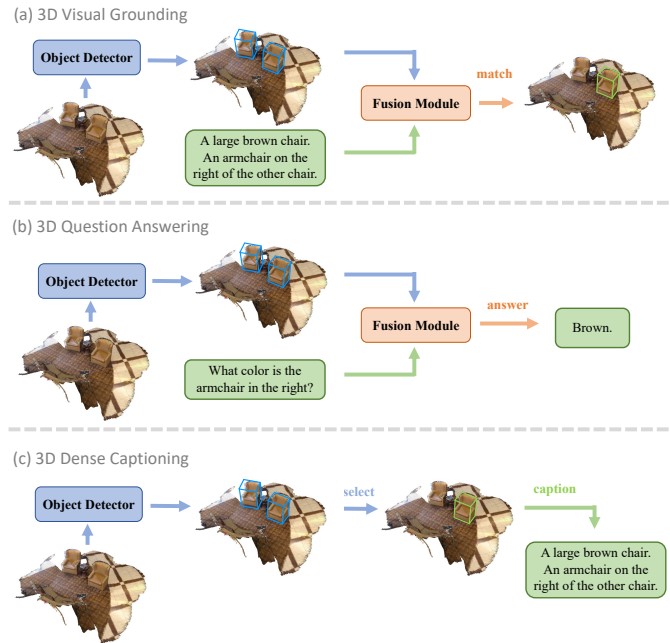


Figure 1: Relationship between 3D vision-language tasks. Firstly, all the tasks rely heavily on the object detector to locate object in the scene. Secondly, 3D vision-language tasks require an effective fusion module to understand the connection between point cloud and language.

joint multimodal representation is to adopt the pre-training plus fine-tuning paradigm, whose effectiveness have been demonstrated by the remarkable success in 2D vision-language pre-training [2, 10, 24, 25, 36, 46]. Existing works on 3D vision-language pre-training are still limited, which motivates us to introduce this paradigm into semantic 3D scene understanding in an appropriate way. However, 3D vision-language pre-training differs from pre-training in NLP and 2D vision-language tasks since point cloud data is introduced [15]. The task-agnostic objectives designed in previous works cannot be directly applied to 3D vision-language pre-training due to the gap of downstream tasks. In light of these consideration, it is essential to identify the shared nature across different tasks in semantic 3D scene understanding to further determine the appropriate pre-training model.

*Equal contribution.

✉ Corresponding author: Tao Dai.

Figure 1 provides an intuitive depiction of the relationships among three 3D vision-language tasks. Two key observations emerge from the comparison of these tasks. Firstly, all of these tasks rely heavily on the object detection when applying two-stage pipeline models, which is a common practice in semantic 3D scene understanding [7, 11]. Secondly, 3D vision-language tasks require an effective fusion module to enable information interaction between point cloud and language for a deeper understanding of the relationships between objects in the scene, such as the matching stage in the visual grounding [6, 48] and the classification of answers in the question answering [3].

These observations in semantic 3D scene understanding pose several challenges in designing an effective training paradigm for the pre-training model to obtain universal embeddings and achieve better transfer performance flexibly in downstream tasks. Firstly, high-quality bounding boxes are required for object detection, which can be further fed into task-specific heads in downstream tasks. These boxes represent the model’s ability to segment the scene at the object level, as demonstrated by works that use a detection-then-matching pipeline [1, 6, 7, 48]. Secondly, object detection requires the model to distinguish between different objects in the scene, especially when there are many objects similar to the target, which is common in real-life situations [7]. This means the model needs to be able to identify what makes objects distinct in the scene, which is a challenging task that has not yet been fully addressed. Thirdly, the fusion module suffers from the issue that the data come from different modalities are unaligned, as similar to the cross-modal problems in 2D vision language learning [10, 24]. Point cloud features and word token embeddings exist in different spaces, making it challenging for the fusion module to model their interactions.

To this end, we propose 3DVLP: vision-language pre-training with object contrastive learning in semantic 3D scene understanding. 3DVLP is the first pre-training framework that effectively addresses the challenges mentioned above. (1) To obtain better object bounding boxes, we introduce **Object-level IoU-guided Detection** (OID) loss in our pre-training pipeline. Specifically, we leverage visual grounding as the proxy task, as it shares the same objective of localizing high-quality bounding boxes. Additionally, we incorporate Distance IoU (DIoU) loss [50] and label smoothing in the matching stage at the object level to achieve faster convergence and better performance. (2) We further introduce **Object-level Self-Contrastive learning** (OSC) task to distinguish the target object from others. The self-contrastive learning is performed at the object level, where boxes with an IoU higher than a specific threshold are considered positive samples, while others are regarded as negative ones. This self-contrastive loss is designed to bring positive samples closer to each other and far away from the negative ones. (3) To enable fully information interreaction between point cloud and language, we further design **Object-level Cross-Contrastive alignment** (OCC) task as a proxy task to align the unimodal representation across these two modalities. We use a similar IoU filter as in OSC to generate positive and negative samples, which are then fed as inputs to calculate the cross-contrastive loss. The cross-contrastive loss is introduced to pull the embedding of positive samples closer to the anchor feature of the target language description.

Overall, 3DVLP effectively addresses the challenges in semantic 3D scene understanding by proposing these novel proxy tasks that enable effective point-cloud and language information interaction. By introducing OID, OCC, and OSC, our method can achieve state-of-the-art performance on multiple 3D vision-language multimodal tasks. The strong generalization capabilities and short training time for fine-tuning of 3DVLP makes it suitable for a wide range of applications and multiple tasks.

The contributions of this study are summarized as follows: (1) A 3D vision-language pre-training framework called 3DVLP has been proposed, achieving the unification of the tasks in semantic 3D scene understanding. (2) We introduce Object-level IoU-guided Detection loss into the pre-training pipeline to obtain high-quality bounding boxes for downstream tasks. We also present two proxy tasks at the object level, including the Object-level Cross-Contrastive alignment task and Object-level Self-Contrastive learning task, which facilitate cross-modal alignment and help the model distinguish objects more accurately, respectively. (3) We conduct extensive experiments and empirically demonstrate the effectiveness of our method in semantic 3D scene understanding.

2 RELATED WORK

2.1 Vision-language Pre-training

Vision-language pre-training are proposed to improve the performance in downstream tasks and has been widely explored in recent approaches [10, 22–26, 34, 35]. It is a common practice to pre-train the model with large-scale image-text pair datasets, usually crawled from the web [19, 34]. Borrowed from the insight in NLP tasks [5, 13, 21, 28], various learning objectives are proposed for cross-modal pre-training, enabling the model to capture the relationship between data from different modalities. CLIP [34] aligns the unimodal image representation and language representation by contrastive loss and maximizes similarity of correct pairs. ALBEF [24] and Uniter [10] further apply image-text matching and masked language modeling tasks, enabling model to capture more complex interactions between image and text. Li et al. introduces captioning loss in BLIP [23] to address the issue of noisy image-text pairs, and further bootstraps representation learning from frozen pre-trained unimodal models in BLIP-2 [22].

Pre-training for 3D vision language tasks also suffers from misaligned data across different modalities, leading to difficulties in training the fusion layer [24, 42]. Motivated by the common practice in 2D vision language tasks [24, 47], we introduce contrastive alignment task into 3D vision-language learning and enhance the performance of the pre-training model.

2.2 3D Visual-Language Tasks

Recently, semantic 3D scene understanding has raised great interest and has been widely explored in recent approaches across various tasks, including 3D visual grounding [6, 7, 48], 3D dense captioning [11], and 3D question answering [3].

3D visual grounding aims to locate a region of interest in a scene based on a referring description. Chen et al. [7] introduces the ScanRefer dataset and proposes an end-to-end visual grounding framework. Achlioptas et al. [1] collects two datasets containing

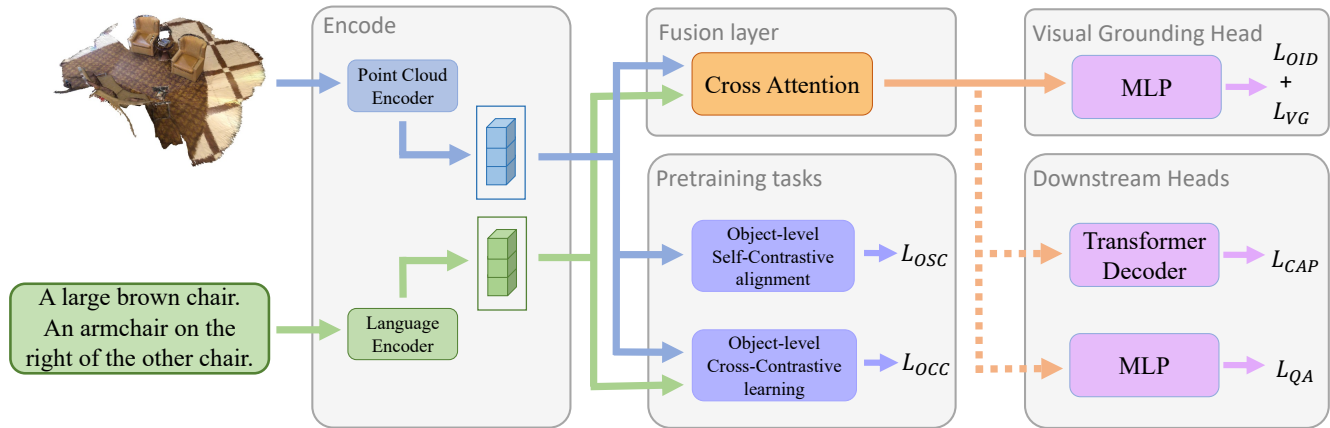


Figure 2: Pipeline of 3DVLP in semantic 3D scene understanding. 3DVLP takes visual grounding as the proxy task and utilizes Object-level IoU-guided Detection (OID) loss to boost the performance of the object detector. We also introduce Object-level Cross-Contrastive alignment task and Object-level Self-Contrastive learning task in the pre-training stage, which facilitate cross-modal alignment and enable the model to distinguish objects more accurately, respectively.

Nr3D and Sr3D with high-quality referential utterances. Most existing methods rely on a detection-then-match pipeline to tackle the grounding task and aim to develop model’s ability to capture the connections between proposal and language description, which is usually implemented by a cross-attention module [39]. For instance, 3DVG-Transformer [48] introduces coordinate-guided contextual aggregation module to enhance proposal generation and cross-modal proposal disambiguation. HAM[9] shifts attention to contextual information and develops both local and global attention module for better end-to-end grounding, while BUTD-DETR[18] presents a DETR-like [51] referential grounding model that incorporates guidance from language, points, and objects. 3D-SPS[30], however, propose the first one-stage end-to-end framework via keypoints selection and mines the cross-modal relationship based on points.

Dense captioning in 3D scene requires model to derive high-quality object bounding box and the corresponding descriptions from point cloud data. Scan2Cap [11] extends the dense captioning task to 3D scenes based on the ScanRefer dataset and establishes a message-passing network to model the connections between objects. SpaCap3D[41] investigates the relative spatiality of objects and build a spatiality-guided transformer to generate captions. Importantly, it designs a object-centric decoder by using a vision token as information carrier of the target object.

3D visual question answering is another vision-language task in which model are expected to generate a correct answer provided with the point cloud and a question. ScanQA[3] collects 41k question-answer pairs and brings the question-answering task into 3D scenes. Besides, it propose a 3D-QA baseline model by casting the answer generation task as a classification problem. FE-3DGQA[49] proposes another datasets and predicts the answer through a token encoding and fusion module based on attention.

Some previous works have made efforts to capture the connection among the tasks above and dig out the basic relationship between object proposals and language expressions. 3DJCG[6] and D3Net [8] model the joint training of 3D dense captioning and 3D visual grounding, thereby boosting the performance of model in both tasks. However, to the best of our knowledge, no framework has leveraged the 3D vision-language pre-training model to improve the performance of downstream tasks. Motivated by the shared nature across different tasks in semantic 3D scene understanding, we summarize the characteristics of a pre-training model and design corresponding proxy tasks to achieve these objectives.

3 METHOD

As illustrated in Figure 2, 3DVLP first encodes point cloud and language data and further applies a cross-attention module to obtain fusion feature for downstream tasks. The training of 3DVLP can be mainly divided into the pre-training stage and the fine-tuning stage. In the pre-training stage, 3DVLP utilizes visual grounding as the proxy task and employs Object-level IoU-guided Detection (OID) loss for high-quality object detection. Additionally, 3DVLP is pre-trained on other designed proxy tasks, including Object-level Cross-Contrastive alignment (OCC) and Object-level Self-Contrastive learning (OSC). In the finetuning stage, we transfer the backbone of 3DVLP to downstream tasks with task-specific heads.

3.1 Object-level IoU-guided Detection Loss

We consider visual grounding as the proxy task since it shares the same objective with the pre-training model of obtaining high-quality proposals. Additionally, we propose Object-level IoU-guided Detection loss to enhance the performance of the object detector, as demonstrated in Fig. 4a.

Specifically, we introduce the Distance IoU (DIoU) loss [50] into the visual grounding pipeline for bounding box regression. Given

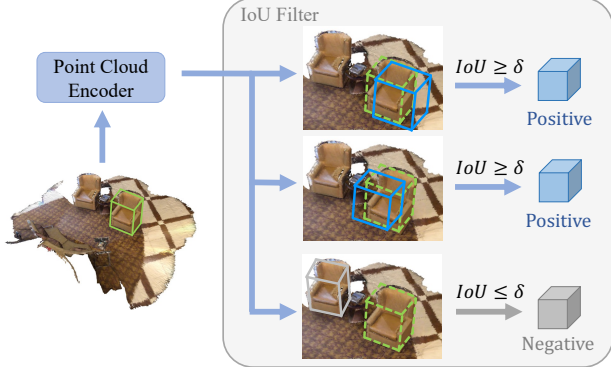


Figure 3: Illustration of the IoU filter in 3DVL. To apply label smoothing and contrastive loss at the object level, proposals with IoU higher than a threshold δ are considered positive samples while others are regarded as the negative ones.

the predicted proposal b_p and ground truth b_{gt} , we calculate the IoU between them and have the following regression loss:

$$\mathcal{L}_{DIOU}(b_p, b_{gt}) = 1 - IoU + \frac{\rho^2(b_p, b_{gt})}{c^2}, \quad (1)$$

where c is the diagonal length of the smallest enclosing box covering the two boxes. However, previous approaches [6, 48] treat the matching stage in visual grounding task as a classification problem and use the proposal with the highest IoU as a supervised label to train the fusion module. In this case, the DIOU loss can only be applied to a single proposal, which weakens its efforts in optimization. Additionally, due to the large number of proposals generated by the detector, there can be multiple boxes pointing to the target object, and these boxes may share similar semantic information, making it difficult to achieve accurate matching with a one-hot label.

Label smoothing is a regularization technique that prevents the model from overconfident prediction [31] and is suitable for addressing such matching problems. Specifically, we apply label smoothing by incorporating an IoU filter into training, as shown in Fig. 3. Given a pre-defined IoU threshold δ and the weight factor ϵ , positive proposals are filtered according to their IoU with the ground truth, and weights are assigned to them based on their total count, denoted by K . The weight of proposal p in the soft label is shown in Equ. (2).

$$y_p = \begin{cases} 1 - \epsilon & \text{if } IoU_p = IoU_{max} \\ \frac{\epsilon}{K} & \text{if } IoU_p \geq \delta \text{ and } IoU_p \neq IoU_{max} \\ 0 & \text{otherwise} \end{cases} \quad (2)$$

We further combine DIOU loss and label smoothing to obtain our OID loss, as demonstrated in Equ. (3).

$$\mathcal{L}_{OID} = \sum_p y_p \cdot \mathcal{L}_{DIOU}(b_p, b_{gt}). \quad (3)$$

3.2 Object-level Cross-contrastive Alignment

As a common practice [6, 48], a cross-modal attention module is applied in semantic 3D scene understanding for feature fusion between language and point cloud embedding. However, it is observed that the data distribution across different modalities is not well-aligned, resulting in insufficient interaction between the embedding of proposals and the language feature. To address this issue, contrastive learning can provide insights for embedding alignment across different distributions. However, naive implementation over proposals is not effective, as semantically similar information from the boxes pointing at the target object conflicts with the optimization target of contrastive loss. This can ultimately lead to a deterioration in performance or even failure to converge.

Based on these observations, we reconsider contrastive learning at the object level and introduce the Object-level Cross-Contrastive alignment (OCC) task to enhance the performance of the cross fusion module, as shown in Fig. 4b. The OCC task is proposed to align the distribution of cross-modal data. Specifically, in the training stage, we introduce the target detection boxes of real objects and select all the predicted boxes with IoU greater than a pre-defined threshold as positive samples since they semantically point to the target object and should have similar features. The remaining predicted boxes are considered negative samples, representing the proposals of other objects or background. We then align the features of positive samples with the language embedding and push the features of negative samples away with the contrastive loss to achieve better cross-modal understanding.

Formally, we have the following contrastive loss, which serves as the loss function for our OCC task.

$$\mathcal{L}_{OCC} = -\frac{1}{2} \mathbb{E}_{(b_{gt}, T) \sim D} \left[\log \frac{\sum_{p \in P_{pos}} \exp(s(H_p, T))}{\sum_{\hat{p} \in P_{pos} \cup P_{neg}} \exp(s(H_{\hat{p}}, T))} + \log \frac{\sum_{p \in P_{pos}} \exp(s(T, H_p))}{\sum_{\hat{p} \in P_{pos} \cup P_{neg}} \exp(s(T, H_{\hat{p}}))} \right], \quad (4)$$

where H_p represents the embedding of proposal p , and T denotes the language embedding. Given \mathbb{I} as the indicator function, $IoU(\cdot, \cdot)$ as the IoU score between two boxes, and δ as the IoU threshold, we have $P_{pos} = \{p | IoU(b_p, b_{gt}) \geq \delta\}$ as the set of proposals containing positive samples while $P_{neg} = \{p | IoU(b_p, b_{gt}) < \delta\}$ containing the negative ones. $s(\cdot, \cdot)$ represents the similarity score function for measuring the similarity between two types of features, such as by performing a dot product operation.

Note that the threshold δ determines how close positive samples should be to align with the language embedding. Specifically, when $\delta = IoU_{max}$, Equ. (4) only considers the proposal with the highest IoU to be the positive sample and reverts to the original formula of traditional pairwise contrastive loss.

3.3 Object-level Self-contrastive Learning

In semantic 3D scene understanding, the presence of similar objects in the scene can significantly affect the model's matching performance. Therefore, a well-designed pre-training model should be capable of accurately distinguishing between objects in the scene and understanding what makes them similar or different. Achieving

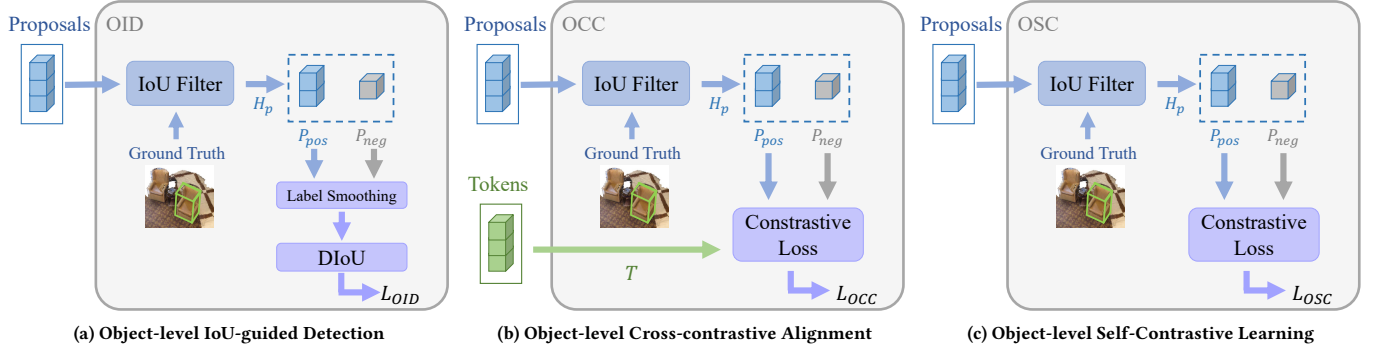


Figure 4: Illustration of Object-level IoU-guided Detection (OID) loss, Object-level Cross-contrastive alignment (OCC) and Object-level Self-Contrastive learning (OSC) pre-training tasks. All the modules utilize a IoU filter to select positive proposals.

this is a fundamental task that challenges the model’s overall understanding of the scene. To address this issue, one effective approach is to utilize contrastive loss that incentivizes the model to capture features that differentiate objects. This can lead to an improved matching performance and enhance the model’s ability to identify the target object based on the given description. Similarly, we require an object-level self-contrastive loss instead of the pairwise loss to effectively differentiate between objects and improve the model’s semantic understanding of the scene.

Therefore, we introduce the Object-level Self-Contrastive learning (OSC) task for object detection, as shown in Fig. 4c. The OSC task is proposed for unimodal point cloud data and aims to optimize the embedding generated by the point cloud encoder. Based on the idea in OCC task, we utilize the IoU threshold to select positive samples and negative ones for self contrastive learning. By optimizing the self-contrastive loss, 3DVLP encourages the features of the boxes targeting the ground truth object to be as dissimilar as possible from those of other boxes, thereby enabling the fusion module to distinguish different objects easily.

Following Equ. (4), we replace the language embedding with the embedding of proposals to obtain the corresponding contrastive loss for OSC module, as shown in Equ. (5).

$$\mathcal{L}_{OSC} = -\mathbb{E}_{b_{gt} \sim D} \left[\log \frac{\sum_{p, \hat{p} \in P_{pos}} \exp(s(H_p, H_{\hat{p}}))}{\sum_{p, \hat{p} \in P_{pos} \cup P_{neg}} \exp(s(H_p, H_{\hat{p}}))} \right]. \quad (5)$$

3.4 Heads for Downstream Tasks

3.4.1 3D Visual Grounding. 3D visual grounding task involves matching a language description to the corresponding detection box in a given point cloud data of the scene. As a common practice, we model this matching task as a classification problem by directly using the proposal features obtained from the cross-modal attention module, transforming it into a n -class classification task, where n represents the total number of predicted boxes. The classification label serves as the supervision information to optimize the MLP matching module using cross-entropy loss:

$$\mathcal{L}_{VG} = -\frac{1}{|P_m|} \sum_{p_m \in P_m} y_m \cdot \log(p_m), \quad (6)$$

where $|P_m|$ denotes the total number of the proposals, p_m represents the matching score calculated for each proposal, and y_m represents the corresponding weight in the classification label.

3.4.2 3D Dense Captioning. 3D dense captioning task involves generating corresponding descriptions for all objects in a given scene. To implement the captioning module, we follow the design in SpaCap3D [41] and insert a special visual token with proposal embedding into the initial position of the sequence, which interacts with the word tokens in the attention module. We can then divide this task into training and inference stages.

In the training stage, as we already have specific information about the ground truth, we associate each real object with the nearest proposal and then use the corresponding embedding to perform captioning. We use the natural description as the supervised label to optimize the captioning module through cross-entropy loss:

$$\mathcal{L}_{CAP} = -\frac{1}{|P_{cap}|} \sum_{p_{cap} \in P_{cap}} y_{cap} \cdot \log(p_{cap}), \quad (7)$$

where P_{cap} represents the score vector of each word in the sequence, while p_{cap} and y_{cap} denote the prediction vector and the ground truth label of a single word, respectively. Note that we also utilize masked language modeling [13] in dense captioning.

In the inference stage, we need to perform captioning on all the objects in the scene. Therefore, all the proposals obtained from the point cloud encoder are fed into the Non-Maximum Suppression filter and then into the captioning module as queries.

3.4.3 3D Question Answering. 3D question answering task involves providing answers to questions about objects given the scene data. Following ScanQA [3], we simplify this task into a multi-class classification task for all possible answers. We count and deduplicate all answers, and consider each remaining answer as an output class in the classification task.

Specifically, a lightweight MLP is adopted to predict the score for each answer based on the fusion feature, and the answer with the highest score is selected as the final answer. Cross-entropy loss is used as the loss function to optimize the answering module:

$$\mathcal{L}_{QA} = -\frac{1}{|P_{qa}|} \sum_{p_{qa} \in P_{qa}} y_{qa} \cdot \log(p_{qa}), \quad (8)$$

where p_{qa} represents the answer score computed by the model, and y_{qa} represents the ground truth label.

4 EXPERIMENT

4.1 Datasets and Implementation Details

Visual Grounding Dataset: We select the benchmark dataset ScanRefer [7] for visual grounding task. It consists of 800 3D scenes from the ScanNet dataset [12], each annotated with bounding boxes around objects of interest and corresponding text descriptions. To evaluate our results, we employed two evaluation metrics: IoU@0.25 and IoU@0.5, which measure the percentage of times the proposals have an IoU greater than the threshold.

Dense Captioning Dataset: We conduct experiments on Scan2Cap dataset [11] to evaluate the effectiveness of our method for the dense captioning task. Similar to Scan2Cap, we jointly measure the quality of the generated model with captioning metrics including CIDEr [40], BIEU-4 [32], METEOR [4] and ROUGE [27], cited as C, B-4, M and R, respectively. We combine the metrics above with an IOU threshold and adopt the $m@kIoU$ metric:

$$m@kIoU = \frac{1}{N} \sum_{i=1}^N m_i \cdot \mathbb{I}(IoU \geq k) \quad (9)$$

where m represents the captioning metric, k is the threshold of IoU and \mathbb{I} stands for the indicator function.

Question Answering Dataset: We perform a quantitative evaluation on the question answering tasks over the ScanQA dataset [3]. The ScanQA dataset consists of 41363 questions and 32337 unique answers from 800 scenes derived from the ScanNet scenes. Following the evaluation methodology in [3], EM@1 and EM@10 are used as the evaluation metric. EM@K is the percentage of predictions where the top K predicted answers exactly match any of the ground-truth answers.

4.2 Implementations Details

We first train 3DVLP over the proposed proxy tasks including visual grounding, OCC and OSC in the pre-training stage. We then evaluate our methods on the dense captioning and question answering tasks by transferring the pre-trained model and finetuning it through tasks-specific loss. Similar to 3DJCG[6], we adopt FCOS[37] method to generate the initial object proposals and use 8 sentences per scene in a batch. We train 200 epochs over the grounding task in the pre-training stage. Importantly, we use VoteNet [33] as our point cloud encoder and a frozen BERT[13] as the language encoder to avoid over-fitting on short-length sentences in ScanRefer dataset. For captioning tasks, we use a Transformer decoder with 6 layers and 128 as the hidden size. For QA task, the hidden size of the classification layer is set to be 128 as well. We empirically set the batch size as 8 and adopt the AdamW optimizer [29] with the cosing learning rate decay strategy. The initial learning rate is set to be 0.002 for the detector and $5e-4$ for other modules in the 3DVLP. Codes are implemented by Pytorch and run on a Nvidia 3090 GPU.

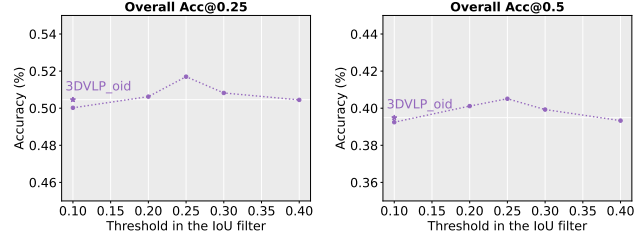


Figure 5: Comparison of the performance when using different threshold in the IoU filter. In addition, we compare a variant of 3DVLP with only OID loss, referred to as 3DVLP_oid.

4.3 Baselines

In 3D visual grounding task, we compare 3DVLP with the benchmark methods including "3D" models [6, 7, 14, 16, 18, 30, 45, 48] and "2D+3D" models [7, 8, 17, 30, 43, 48]. The "3D" models only utilizes raw attributes in point cloud input features, such as the coordinates, colors, and normal vectors of the original point cloud, while "2D+3D" models use 2D multi-view features as additional inputs. In 3D dense captioning task, we choose end-to-end models of this task as the baseline algorithms for comparison. [6, 8, 11, 20, 41]. In 3D question answering task, we compare 3DVLP with ScanQA[3], FE-3DGQA[49] and 2D models with MCAN[44].

4.4 Comparison with State-of-the-art Methods

4.4.1 3D visual grounding task. We present the results of 3D visual grounding in Table 1. The results indicate that 3DVLP performs remarkably well and outperforms the baselines by a large margin. In terms of unique scenes, 3DVLP achieves the highest accuracy in Acc@0.5 and ranks second in Acc@0.25, indicating the significant impact of our OID loss in developing the model's ability to identify high-quality bounding boxes. Previous work solely optimizes the center and size of the proposals, while the introduction of the OID loss improves the quality of proposals targeting the ground truth object.

Furthermore, when comparing multiple and unique metrics, previous works suffers from issues related to the presence of similar objects in the scene, leading to poor matching results. However, the introduction of OSC and OCC tasks in 3DVLP enables it to achieve competitive performance in multiple metrics, showcasing its ability to accurately locate objects in complex scenes. In the overall metric, 3DVLP's performance surpasses the baseline by 0.71% in Acc@0.5 and also ranks second in Acc@0.25, demonstrating its effectiveness in 3D visual grounding.

4.4.2 3D dense captioning task. As presented in Table 2, it is evident that 3DVLP shows excellent transfer performance in dense captioning task. Importantly, the point cloud encoder in 3DVLP extracts universal features that generalize well in dense captioning, enabling 3DVLP to outperform other baselines by a large extent. Specifically, 3DVLP achieves a remarkable improvement of 2.55%, 4.93%, 2.30%, and 2.61% in terms of C@0.25, C@0.5, R@0.25, and

Table 1: Comparison of different methods in 3D visual grounding task. We measure the percentage of the correctly predicted bounding boxes whose IoU with the ground-truth boxes are larger than 0.25 and 0.5, respectively.

Method	Venue	Data	Unique		Multiple		Overall	
			Acc@0.25	Acc@0.5	Acc@0.25	Acc@0.5	Acc@0.25	Acc@0.5
ScanRefer [7]	ECCV2020	3D	67.64	46.19	32.06	21.26	38.97	26.10
TGNN[16]	AAAI2021	2D	68.61	56.80	29.84	23.18	37.37	29.70
InstanceRefer [45]	ICCV2021	3D	77.45	66.83	31.27	24.77	40.23	32.93
FFL-3DOG[14]	ICCV2021	3D	-	67.94	-	25.70	-	34.01
3DVG-Transformer [48]	ICCV2021	3D	77.16	58.47	38.38	28.70	45.90	34.47
3DJCG[6]	CVPR2022	3D	78.75	61.30	40.13	30.08	47.62	36.14
3D-SPS[30]	CVPR2022	3D	81.63	64.77	39.48	29.61	47.65	36.43
BUTD-DETR[18]	ECCV2022	3D	84.20	66.30	46.60	35.10	52.20	39.80
ScanRefer [7]	ECCV2020	2D + 3D	76.33	53.51	32.73	21.11	41.19	27.40
SAT[43]	ICCV2021	2D + 3D	73.21	50.83	37.64	25.16	44.54	30.14
3DVG-Transformer [48]	ICCV2021	2D + 3D	81.93	60.64	39.30	28.42	47.57	34.67
Multi-View Trans [17]	CVPR2022	2D + 3D	77.67	66.45	31.92	25.26	40.80	33.26
3D-SPS[30]	CVPR2022	2D + 3D	<u>84.12</u>	66.72	40.32	29.82	48.82	36.98
3DJCG[6]	CVPR2022	2D + 3D	83.47	64.34	41.39	30.82	49.56	37.33
D3Net [8]	ECCV2022	2D + 3D	-	70.35	-	30.05	-	37.87
3DVLP	-	2D + 3D	85.18	<u>70.04</u>	<u>43.65</u>	<u>33.40</u>	<u>51.70</u>	40.51

Table 2: Comparison of different methods in 3D dense captioning task. We report the result with the percentage of the predicted bounding boxes whose IoU with the ground truth are greater than 0.25 and 0.5.

Method	Venue	C@0.25	B-4@0.25	M@0.25	R@0.25	C@0.5	B-4@0.5	M@0.5	R@0.5
Scan2Cap [11]	CVPR 2021	56.82	34.18	26.29	55.27	39.08	23.32	21.97	44.78
MORE[20]	ECCV 2022	62.91	36.25	26.75	56.33	40.94	22.93	21.66	44.42
SpaCap3D[41]	IJCAI 2022	63.30	36.46	26.71	55.71	44.02	25.26	22.33	45.36
3DJCG [6]	CVPR2022	<u>64.70</u>	<u>40.17</u>	<u>27.66</u>	<u>59.23</u>	<u>49.48</u>	<u>31.03</u>	24.22	50.80
D3Net [8]	ECCV2022	-	-	-	-	46.07	30.29	<u>24.35</u>	<u>51.67</u>
3DVLP	-	67.25	41.30	36.27	61.53	54.41	34.10	34.34	54.28

Table 3: Comparison of different methods in 3D question answering task. The results are presented with the percentage of predictions where the top K predicted answers exactly match any of the ground-truth answers. We also report Acc@0.25 and Acc@0.5 metrics, similar to the visual grounding metrics.

Method	EM@1	EM@10	Acc@0.25	Acc@0.5
VoteNet [33]+MCAN	17.33	45.54	-	-
ScanRefer [7]+MCAN	18.59	46.76	23.53	11.76
ScanQA[3]	21.05	51.23	24.96	15.42
FE-3DGQA[49]	<u>22.26</u>	<u>54.51</u>	<u>26.62</u>	<u>18.83</u>
3DVLP	24.03	57.91	33.38	26.12

Table 4: Ablation analysis. We provide quantitative results of the overall accuracy in visual grounding and the metric under IoU=0.5 setting in dense captioning.

Module			Visual Grounding		Dense Captioning			
OID	OCC	OSC	Acc@0.25	Acc@0.5	C@0.5	B-4@0.5	M@0.5	R@0.5
			50.59	37.96	53.12	31.90	33.93	52.27
✓			50.46	39.49	52.91	33.91	34.28	54.08
	✓		51.15	38.44	53.24	32.79	33.98	52.99
		✓	50.91	38.28	51.41	32.93	34.00	52.94
✓	✓	✓	51.70	40.51	54.41	34.10	34.34	54.28

R@0.5, respectively. Moreover, the results show that 3DVLP outperforms the second baseline by 8.61% in M@0.25 and 9.99% in M@0.5. Among various evaluation metrics, METEOR focuses on capturing the semantic similarity and fluency between the output and the ground truth, thereby indicating the generalization ability of the encoder in 3DVLP. In comparison to SpaCap3D, which shares the same decoder architecture as 3DVLP, we observe a significant performance boost resulting from the pre-training backbone, thus demonstrating the effectiveness of the proxy tasks designed in the pre-training stage.

4.4.3 3D question answering task. From the results in Table 3, the most striking observation emerging from the comparison is that 3DVLP consistently outperforms other methods and improves the performance in the question answering task. For example, 3DVLP achieves approximately 1.7%-2.4% improvement in EM@1 and EM@10 compared to the baseline. Moreover, it can be concluded that question answering benefits from the pre-training model when compared to ScanQA, as 3DVLP utilizes the same classification head. Furthermore, 3DVLP provides a boost by 6.76% and 7.23% in Acc@0.25 and Acc@0.5, respectively. However, it is noteworthy that the results are lower than those achieved in visual grounding, primarily due to the inclusion of the task-specific loss in the question answering task.

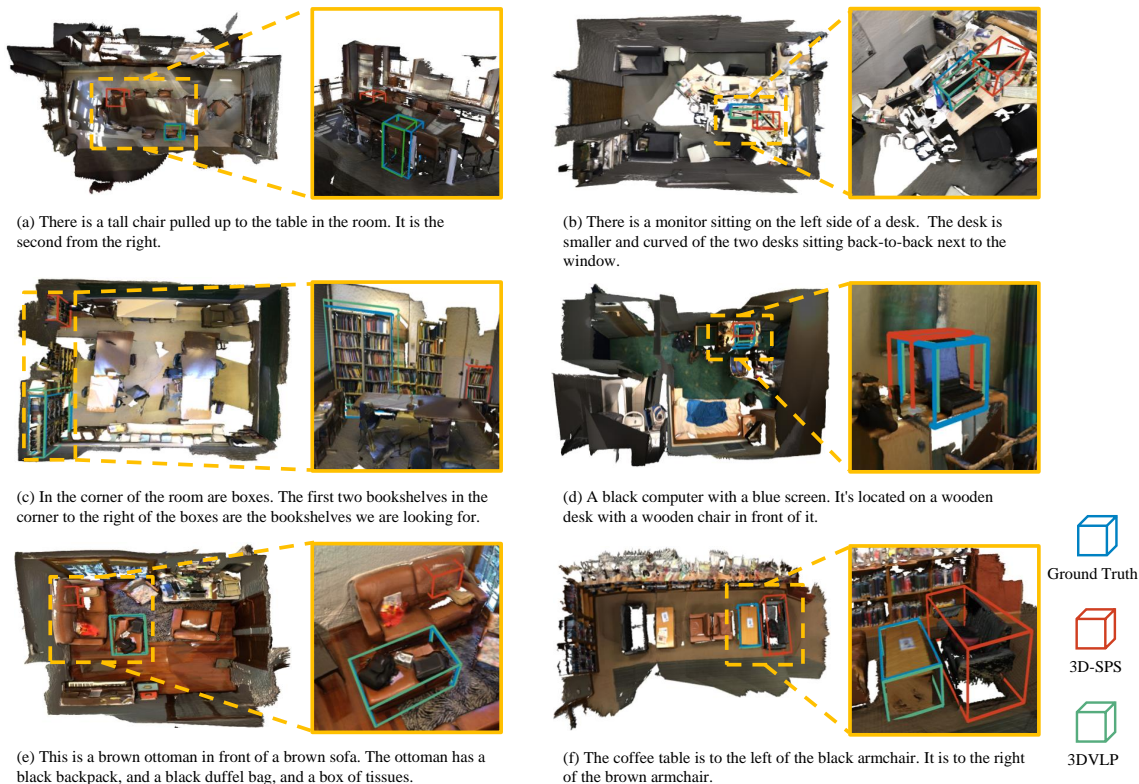


Figure 6: Qualitative results of 3DVLP and 3D-SPS. We mark the ground truth in blue, 3D-SPS in red and 3DVLP in green.

4.5 Ablation Study

Does the OID loss and the designed proxy tasks benefit downstream tasks? We conducted a series of ablation experiments to investigate the contribution of each module in 3DVLP. The results in Table 4 demonstrate that both visual grounding and dense captioning tasks benefit from each proposed module. In visual grounding, the OID loss significantly improves the quality of the predicted bounding boxes, thereby enhancing $\text{Acc}@0.5$ to a large degree. Furthermore, neither the introduction of OSC nor OCC provides a remarkable boost in $\text{Acc}@0.25$, indicating the superiority of modeling optimization at the object level in complex scenes. In dense captioning, the improvement of the model is consistent with that in visual grounding by combining the modules together.

Is the improvement in OSC and OCC sensitive to the threshold used the IoU filter? To have a better understanding of the threshold δ used in the IoU filter, we estimate the results of the overall Acc in visual grounding with the varying δ . Moreover, we also include 3DVLP with only OID loss as a base variant, referred as 3DVLP_{oid}. As shown in Fig. 5, the performance obviously improves when increasing the threshold from 0.1 to 0.25. This is because proposals targeting other objects can be incorrectly considered as positive samples and thus mislead the training optimization when using a low threshold. However, we further increase the threshold and observe that the improvement is not consistent. The performance drops with a large threshold since model will regard

proposals that are not good enough as negative samples, resulting in semantic divergence. This is similar to what happens with the traditional pairwise contrastive loss. Therefore, based on our results, we believe that selecting a threshold of 0.25 in the IoU filter is a reasonable tradeoff.

4.6 Qualitative Results

To further explore how 3DVLP improves the performance in visual grounding, we provide the comparison results with 3D-SPS as shown in Figure 6. Figure 6(d) indicates that OID loss contribute to more high-quality bounding boxes, thereby boosting the performance. Additionally, these examples demonstrate that 3DVLP has a better understanding of the relationship between scene and language as a result of incorporating OSC and OCC, leading to more reliable visual grounding results.

5 CONCLUSION

This paper investigates the shared nature across different tasks in semantic 3D scene understanding and proposes a contrastive 3D vision-language pre-training framework named 3DVLP, which transfers flexibly in the downstream tasks. 3DVLP introduces the object-level IoU-guided detection loss to obtain high-quality proposals, aligns the point cloud representation and language representation by training over object-level cross-contrastive alignment task and develops its ability to distinguish different objects in the

scene through object-level self-contrastive learning task, which defines a new paradigm for the 3D vision-language pre-training model. Comprehensive experiments reveal the generalization ability and superiority of 3D-VLP over all downstream tasks in semantic 3D scene understanding, leading to a new state-of-the-art performance. Future work needs to focus on dealing with the fusion of point cloud and language, desirably about the full interaction of multi-level information.

REFERENCES

- [1] Panos Achlioptas, Ahmed Abdelreheem, Fei Xia, Mohamed Elhoseiny, and Leonidas Guibas. 2020. Referit3d: Neural listeners for fine-grained 3d object identification in real-world scenes. In *Computer Vision–ECCV 2020: 16th European Conference, Glasgow, UK, August 23–28, 2020, Proceedings, Part I 16*. Springer, 422–440.
- [2] Jean-Baptiste Alayrac, Jeff Donahue, Pauline Luc, Antoine Miech, Iain Barr, Yana Hasson, Karel Lenc, Arthur Mensch, Katherine Millican, Malcolm Reynolds, et al. 2022. Flamingo: a visual language model for few-shot learning. *Advances in Neural Information Processing Systems* 35 (2022), 23716–23736.
- [3] Daichi Azuma, Taiki Miyanishi, Shuhei Kurita, and Motoaki Kawanabe. 2022. ScanQA: 3D question answering for spatial scene understanding. In *Proceedings of the IEEE/CVF Conference on Computer Vision and Pattern Recognition*. 19129–19139.
- [4] Satangee Banerjee and Alon Lavie. 2005. METEOR: An automatic metric for MT evaluation with improved correlation with human judgments. In *Proceedings of the acl workshop on intrinsic and extrinsic evaluation measures for machine translation and/or summarization*. 65–72.
- [5] Tom Brown, Benjamin Mann, Nick Ryder, Melanie Subbiah, Jared D Kaplan, Prafulla Dhariwal, Arvind Neelakantan, Pranav Shyam, Girish Sastry, Amanda Askell, et al. 2020. Language models are few-shot learners. *Advances in neural information processing systems* 33 (2020), 1877–1901.
- [6] Daigang Cai, Lichen Zhao, Jing Zhang, Lu Sheng, and Dong Xu. 2022. 3djcg: A unified framework for joint dense captioning and visual grounding on 3d point clouds. In *Proceedings of the IEEE/CVF Conference on Computer Vision and Pattern Recognition*. 16464–16473.
- [7] Dave Zhenyu Chen, Angel X Chang, and Matthias Nießner. 2020. Scanrefer: 3d object localization in rgb-d scans using natural language. In *Computer Vision–ECCV 2020: 16th European Conference, Glasgow, UK, August 23–28, 2020, Proceedings, Part XX*. Springer, 202–221.
- [8] Dave Zhenyu Chen, Qirui Wu, Matthias Nießner, and Angel X Chang. 2021. D3Net: a speaker-listener architecture for semi-supervised dense captioning and visual grounding in RGB-D scans. *arXiv preprint arXiv:2112.01551* (2021).
- [9] Jiaming Chen, Weixin Luo, Xiaolin Wei, Lin Ma, and Wei Zhang. 2022. HAM: Hierarchical Attention Model with High Performance for 3D Visual Grounding. *arXiv preprint arXiv:2210.12513* (2022).
- [10] Yen-Chun Chen, Linjie Li, Licheng Yu, Ahmed El Kholy, Faisal Ahmed, Zhe Gan, Yu Cheng, and Jingjing Liu. 2020. Uniter: Universal image-text representation learning. In *Computer Vision–ECCV 2020: 16th European Conference, Glasgow, UK, August 23–28, 2020, Proceedings, Part XXX*. Springer, 104–120.
- [11] Zhenyu Chen, Ali Gholami, Matthias Nießner, and Angel X Chang. 2021. Scan2cap: Context-aware dense captioning in rgb-d scans. In *Proceedings of the IEEE/CVF Conference on Computer Vision and Pattern Recognition*. 3193–3203.
- [12] Angela Dai, Angel X Chang, Manolis Savva, Maciej Halber, Thomas Funkhouser, and Matthias Nießner. 2017. Scannet: Richly-annotated 3d reconstructions of indoor scenes. In *Proceedings of the IEEE conference on computer vision and pattern recognition*. 5828–5839.
- [13] Jacob Devlin, Ming-Wei Chang, Kenton Lee, and Kristina Toutanova. 2018. Bert: Pre-training of deep bidirectional transformers for language understanding. *arXiv preprint arXiv:1810.04805* (2018).
- [14] Mingtao Feng, Zhen Li, Qi Li, Liang Zhang, Xiangdong Zhang, Guangming Zhu, Hui Zhang, Yaonan Wang, and Ajmal Mian. 2021. Free-form description guided 3d visual graph network for object grounding in point cloud. In *Proceedings of the IEEE/CVF International Conference on Computer Vision*. 3722–3731.
- [15] Yulan Guo, Hanyun Wang, Qingyong Hu, Hao Liu, Li Liu, and Mohammed Bennamoun. 2020. Deep learning for 3d point clouds: A survey. *IEEE transactions on pattern analysis and machine intelligence* 43, 12 (2020), 4338–4364.
- [16] Pin-Hao Huang, Han-Hung Lee, Hwann-Tzong Chen, and Tyng-Luh Liu. 2021. Text-guided graph neural networks for referring 3d instance segmentation. In *Proceedings of the AAAI Conference on Artificial Intelligence*, Vol. 35. 1610–1618.
- [17] Shijia Huang, Yilun Chen, Jiaya Jia, and Liwei Wang. 2022. Multi-view transformer for 3d visual grounding. In *Proceedings of the IEEE/CVF Conference on Computer Vision and Pattern Recognition*. 15524–15533.
- [18] Ayush Jain, Nikolaos Gkanatsios, Ishita Mediratta, and Katerina Fragkiadaki. 2022. Bottom up top down detection transformers for language grounding in images and point clouds. In *Computer Vision–ECCV 2022: 17th European Conference, Tel Aviv, Israel, October 23–27, 2022, Proceedings, Part XXXVI*. Springer, 417–433.
- [19] Chao Jia, Yinfei Yang, Ye Xia, Yi-Ting Chen, Zarana Parekh, Hieu Pham, Quoc Le, Yun-Hsuan Sung, Zhen Li, and Tom Duerig. 2021. Scaling up visual and vision-language representation learning with noisy text supervision. In *International Conference on Machine Learning*. PMLR, 4904–4916.
- [20] Yang Jiao, Shaoxiang Chen, Zequn Jie, Jingjing Chen, Lin Ma, and Yu-Gang Jiang. 2022. More: Multi-order relation mining for dense captioning in 3d scenes. In *Computer Vision–ECCV 2022: 17th European Conference, Tel Aviv, Israel, October 23–27, 2022, Proceedings, Part XXXV*. Springer, 528–545.
- [21] Zhenzhong Lan, Mingda Chen, Sebastian Goodman, Kevin Gimpel, Piyush Sharma, and Radu Soricut. 2019. Albert: A lite bert for self-supervised learning of language representations. *arXiv preprint arXiv:1909.11942* (2019).
- [22] Junnan Li, Dongxu Li, Silvio Savarese, and Steven Hoi. 2023. BLIP-2: Bootstrapping Language-Image Pre-training with Frozen Image Encoders and Large Language Models. *arXiv preprint arXiv:2301.12597* (2023).
- [23] Junnan Li, Dongxu Li, Caiming Xiong, and Steven Hoi. 2022. Blip: Bootstrapping language-image pre-training for unified vision-language understanding and generation. In *International Conference on Machine Learning*. PMLR, 12888–12900.
- [24] Junnan Li, Ramprasaath Selvaraju, Akhilesh Gotmare, Shafiq Joty, Caiming Xiong, and Steven Chu Hong Hoi. 2021. Align before fuse: Vision and language representation learning with momentum distillation. *Advances in neural information processing systems* 34 (2021), 9694–9705.
- [25] Liunan Harold Li, Mark Yatskar, Da Yin, Cho-Jui Hsieh, and Kai-Wei Chang. 2019. Visualbert: A simple and performant baseline for vision and language. *arXiv preprint arXiv:1908.03557* (2019).
- [26] Xiujun Li, Xi Yin, Chunyuan Li, Pengchuan Zhang, Xiaowei Hu, Lei Zhang, Lijuan Wang, Houdong Hu, Li Dong, Furu Wei, et al. 2020. Oscar: Object-semantics aligned pre-training for vision-language tasks. In *Computer Vision–ECCV 2020: 16th European Conference, Glasgow, UK, August 23–28, 2020, Proceedings, Part XXX 16*. Springer, 121–137.
- [27] Chin-Yew Lin. 2004. Rouge: A package for automatic evaluation of summaries. In *Text summarization branches out*. 74–81.
- [28] Yinhan Liu, Myle Ott, Naman Goyal, Jingfei Du, Mandar Joshi, Danqi Chen, Omer Levy, Mike Lewis, Luke Zettlemoyer, and Veselin Stoyanov. 2019. Roberta: A robustly optimized bert pretraining approach. *arXiv preprint arXiv:1907.11692* (2019).
- [29] Ilya Loshchilov and Frank Hutter. 2017. Decoupled weight decay regularization. *arXiv preprint arXiv:1711.05101* (2017).
- [30] Junyu Luo, Jiahui Fu, Xianghao Kong, Chen Gao, Haibing Ren, Hao Shen, Huaxia Xia, and Si Liu. 2022. 3d-sps: Single-stage 3d visual grounding via referred point progressive selection. In *Proceedings of the IEEE/CVF Conference on Computer Vision and Pattern Recognition*. 16454–16463.
- [31] Rafael Müller, Simon Kornblith, and Geoffrey E Hinton. 2019. When does label smoothing help? *Advances in neural information processing systems* 32 (2019).
- [32] Kishore Papineni, Salim Roukos, Todd Ward, and Wei-Jing Zhu. 2002. Bleu: a method for automatic evaluation of machine translation. In *Proceedings of the 40th annual meeting of the Association for Computational Linguistics*. 311–318.
- [33] Charles R Qi, Or Litany, Kaiming He, and Leonidas J Guibas. 2019. Deep hough voting for 3d object detection in point clouds. In *Proceedings of the IEEE/CVF International Conference on Computer Vision*. 9277–9286.
- [34] Alec Radford, Jong Wook Kim, Chris Hallacy, Aditya Ramesh, Gabriel Goh, Sandhini Agarwal, Girish Sastry, Amanda Askell, Pamela Mishkin, Jack Clark, et al. 2021. Learning transferable visual models from natural language supervision. In *International conference on machine learning*. PMLR, 8748–8763.
- [35] Weijie Su, Xizhou Zhu, Yue Cao, Bin Li, Lewei Lu, Furu Wei, and Jifeng Dai. 2019. Vl-bert: Pre-training of generic visual-linguistic representations. *arXiv preprint arXiv:1908.08530* (2019).
- [36] Hao Tan and Mohit Bansal. 2019. Lxmert: Learning cross-modality encoder representations from transformers. *arXiv preprint arXiv:1908.07490* (2019).
- [37] Zhi Tian, Chunhua Shen, Hao Chen, and Tong He. 2019. Fcos: Fully convolutional one-stage object detection. In *Proceedings of the IEEE/CVF international conference on computer vision*. 9627–9636.
- [38] Laurens Van der Maaten and Geoffrey Hinton. 2008. Visualizing data using t-SNE. *Journal of machine learning research* 9, 11 (2008).
- [39] Ashish Vaswani, Noam Shazeer, Niki Parmar, Jakob Uszkoreit, Llion Jones, Aidan N Gomez, Łukasz Kaiser, and Illia Polosukhin. 2017. Attention is all you need. *Advances in neural information processing systems* 30 (2017).
- [40] Ramakrishna Vedantam, C Lawrence Zitnick, and Devi Parikh. 2015. Cider: Consensus-based image description evaluation. In *Proceedings of the IEEE conference on computer vision and pattern recognition*. 4566–4575.
- [41] Heng Wang, Chaoyi Zhang, Jianhui Yu, and Weidong Cai. 2022. Spatiality-guided transformer for 3d dense captioning on point clouds. *arXiv preprint arXiv:2204.10688* (2022).
- [42] Jinyu Yang, Jiali Duan, Son Tran, Yi Xu, Sampath Chanda, Liqun Chen, Belinda Zeng, Trishul Chilimbi, and Junzhou Huang. 2022. Vision-language pre-training with triple contrastive learning. In *Proceedings of the IEEE/CVF Conference on Computer Vision and Pattern Recognition*. 15671–15680.

- [43] Zhengyuan Yang, Songyang Zhang, Liwei Wang, and Jiebo Luo. 2021. Sat: 2d semantics assisted training for 3d visual grounding. In *Proceedings of the IEEE/CVF International Conference on Computer Vision*. 1856–1866.
- [44] Zhou Yu, Jun Yu, Yuhao Cui, Dacheng Tao, and Qi Tian. 2019. Deep modular co-attention networks for visual question answering. In *Proceedings of the IEEE/CVF conference on computer vision and pattern recognition*. 6281–6290.
- [45] Zhihao Yuan, Xu Yan, Yinghong Liao, Ruimao Zhang, Sheng Wang, Zhen Li, and Shuguang Cui. 2021. Instancerefer: Cooperative holistic understanding for visual grounding on point clouds through instance multi-level contextual referring. In *Proceedings of the IEEE/CVF International Conference on Computer Vision*. 1791–1800.
- [46] Xiaohua Zhai, Xiao Wang, Basil Mustafa, Andreas Steiner, Daniel Keysers, Alexander Kolesnikov, and Lucas Beyer. 2022. Lit: Zero-shot transfer with locked-image text tuning. In *Proceedings of the IEEE/CVF Conference on Computer Vision and Pattern Recognition*. 18123–18133.
- [47] Han Zhang, Jing Yu Koh, Jason Baldrige, Honglak Lee, and Yinfei Yang. 2021. Cross-modal contrastive learning for text-to-image generation. In *Proceedings of the IEEE/CVF conference on computer vision and pattern recognition*. 833–842.
- [48] Lichen Zhao, Daigang Cai, Lu Sheng, and Dong Xu. 2021. 3DVG-Transformer: Relation modeling for visual grounding on point clouds. In *Proceedings of the IEEE/CVF International Conference on Computer Vision*. 2928–2937.
- [49] Lichen Zhao, Daigang Cai, Jing Zhang, Lu Sheng, Dong Xu, Rui Zheng, Yinjie Zhao, Lipeng Wang, and Xibo Fan. 2022. Towards Explainable 3D Grounded Visual Question Answering: A New Benchmark and Strong Baseline. *IEEE Transactions on Circuits and Systems for Video Technology* (2022).
- [50] Zhaohui Zheng, Ping Wang, Wei Liu, Jinze Li, Rongguang Ye, and Dongwei Ren. 2020. Distance-IoU loss: Faster and better learning for bounding box regression. In *Proceedings of the AAAI conference on artificial intelligence*, Vol. 34. 12993–13000.
- [51] Xizhou Zhu, Weijie Su, Lewei Lu, Bin Li, Xiaogang Wang, and Jifeng Dai. 2020. Deformable detr: Deformable transformers for end-to-end object detection. *arXiv preprint arXiv:2010.04159* (2020).

Appendix

A OVERVIEW

In Section B, we provide more details of the datasets used in the downstream tasks. In Section C, we conduct the ablation study in 3D question answering and show the effect of each module in 3DVLP. In Section D, we compare 3DVLP with variant that train from scratch to verify the effectiveness and superiority of the pre-training stage. In Section F, we provide the t-SNE [38] visualization of proposal features in the scene from 3DVLP and variant without OID, OCC and OSC. In Section E, we show more qualitative results in 3D dense captioning task.

B DATASET DETAILS

To benchmark the performance in the downstream tasks, we select different datasets in the experiments and describe their detailed information below.

ScanRefer[7]. ScanRefer is a large-scale benchmark dataset designed for 3D object localization and referred object segmentation in real-world scenes. The dataset consists of textual descriptions of objects present in the scene and their corresponding 3D bounding boxes. The main objective of the dataset is to enhance the performance of 3D object detection and recognition in real-world scenarios by providing a benchmark for models that can understand natural language descriptions of objects and their spatial relationships. The dataset comprises a total of 51,583 descriptions of 11,046 objects, which have been divided into train/val/test sets with 36,655, 9,508, and 2,068 samples, respectively. Additionally, ScanRefer categorizes the data into two subsets: "unique" and "multiple." The "unique" subset contains grounding data with only a single object of its class in the scene, while the "multiple" subset contains data with more than one object of a particular class in the scene.

Scan2Cap [11]. Scan2Cap is a dataset designed for generating natural language descriptions of indoor scenes from 3D point cloud data. The primary objective of this dataset is to provide a benchmark for models that can generate natural language descriptions of indoor scenes using 3D point cloud data. The dataset is highly useful for evaluating the effectiveness of different techniques for combining computer vision and natural language processing to generate coherent and accurate descriptions of indoor scenes. To simplify the problem, Scan2Cap truncates descriptions longer than 30 tokens in ScanRefer and adds two special tokens, namely SOS and EOS, to indicate the start and end of the description. Additionally, Scan2Cap follows the same data division as ScanRefer, dividing the 36,665 and 9,508 samples into train and validation sets, respectively.

ScanQA [3]. The ScanQA dataset is a benchmark dataset designed for visual question answering (VQA) in 3D scenes. Based on the ScanNet dataset, it provides high-quality 3D scanning data of indoor scenes with corresponding questions and answers. The dataset covers a wide range of object categories, making it a challenging benchmark for VQA models. ScanQA contains a total of 41,363 questions and 58,191 answers, including 32,337 unique questions and 16,999 unique answers. It follows the same training, validation, and test set splits as in ScanRefer.

Table 5: Ablation analysis in question answering. We report the percentage of exactly matched predictions.

Module			Question Answering	
OID	OCC	OSC	EM@1	EM@10
			23.23	56.66
✓			22.58	55.94
	✓		23.80	57.88
		✓	24.75	57.24
✓	✓	✓	24.03	57.91

C ABLATION ANALYSIS IN 3D QUESTION ANSWERING

We conducted ablation experiments in 3D question answering and report the results in Table 5. As shown in the results, the OCC and OSC modules provide a positive boost, while the OID module results in a slight drop in performance. We hypothesize that this is because adding alone the OID loss does not enable the model to handle the complex relationship in the scene according to the questions.

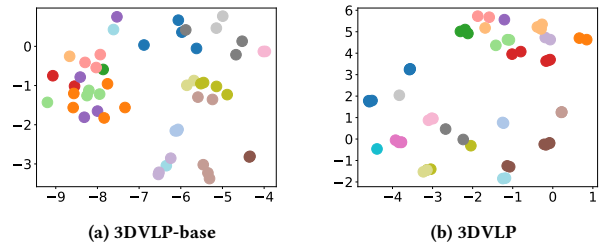


Figure 7: t-SNE visualization of proposal features in the scene. 3DVLP-base is the variant of 3DVLP that does not include OID, OSC and OCC modules.

D COMPARISON WITH TRAINING FROM SCRATCH

We conduct extensive experiments and provide comparison results between 3DVLP and training from scratch in downstream tasks to evaluate the effectiveness of the pre-training stage. Since 3DVLP is fine-tuned in downstream tasks for 20 epochs, we used its variants that are trained from scratch for 20 epochs and trained from scratch until full convergence as baselines, denoted as scratch-20 and scratch-full, respectively.

As shown in Table 6, the results demonstrate that the pre-training stage over the proxy tasks provides a significant boost in performance. When comparing with 3DVLP with scratch-20, we observe that 3DVLP shows superiority in all metrics with the same training time. The training in the pre-training stage enhances the performance by 0.5-6% in captioning metrics and 2-4% in QA metrics. When comparing with scratch-full, 3DVLP achieves better performance with fewer training times, further verifying the effectiveness

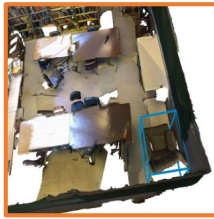
Table 6: Comparison results between 3DVLP and its variants trained from scratch. Specifically, we compare 3DVLP trained from scratch for 20 epochs (denoted as "scratch-20") and 3DVLP trained from scratch until full convergence (denoted as "scratch-full").

Method	Dense Captioning								Question Answering	
	C@0.25	B-4@0.25	M@0.25	R@0.25	C@0.5	B-4@0.5	M@0.5	R@0.5	EM@1	EM@10
scratch-20	59.71	38.89	35.55	59.57	41.38	26.70	32.46	48.01	21.51	53.99
scratch-full	64.14	38.59	35.63	58.94	48.81	30.08	33.29	50.28	22.18	54.04
3DVLP	66.63	40.85	36.12	61.03	54.41	34.10	34.34	54.28	24.03	57.91



Ground Truth:
This is a tv. The tv is suspended on the wall.

3DVLP:
This is a black tv. It is on the wall.



Ground Truth:
This is a brown armchair. It is in a corner of the room.

3DVLP:
This is a brown armchair. It is to the right of a table.



Ground Truth:
This is a brown chair. It is at the end of the table.

3DVLP:
This is a brown chair. It is at the end of the table.

Figure 8: Qualitative results in dense captioning.

of our pre-trained proxy tasks. Interestingly, models mainly develop their captioning ability to high-quality proposals in the late training, as shown by the comparison between scratch-20 and scratch-full.

E MORE QUALITATIVE RESULTS

We provide more qualitative results in dense captioning in Fig 8.

F T-SNE VISUALIZATION OF PROPOSAL FEATURES

We present a t-SNE [38] visualization of proposal features in the scene, as shown in Fig. 7. We use a threshold near the real object

center and filter out the proposals representing the background. Furthermore, we assign labels to the proposals with the nearest real object id. We compare the performance of 3DVLP with its variant that does not include OID, OSC, and OCC modules, namely 3DVLP-base. The visualization shows that the object detector in 3DVLP, with the three proposed modules, is better at distinguishing objects in the scene, which facilitates the optimization of downstream tasks.